PHYSICAL REVIEW B VOLUME 31, NUMBER 11 1 JUNE 1985

Low-temperature magnetization study of U_6X (X=Mn,Fe,Co,Ni) compounds

L. E. DeLong
Department of Physics and Astronomy, University of Kentucky, Lexington, Kentucky 40506

R. P. Guertin* and S. Hasanain†
Department of Physics, Tufts University, Medford, Massachusetts 02155

T. Fariss‡
Department of Physics, University of Virginia, Charlottesville, Virginia 22901

(Received 10 December 1984)

Magnetization and susceptibility measurements have been performed on U_6Fe and U_6Co at temperatures $4\text{ K} \leq T \leq 290\text{ K}$ and applied magnetic fields $10^{-2}\text{ T} \leq H \leq 5\text{ T}$. Low-temperature magnetization measurements at $H = 10^{-2}$ T were also made on U_6Mn, U_6Ni, and $U_6Mn_{0.5}Co_{0.5}$. All of these materials have strongly paramagnetic, weakly-temperature-dependent susceptibilities at $T \leq 290$ K. Low-field magnetization and metallography results provide information concerning the nature of small concentrations of ferromagnetic impurity phases found in all of the samples studied. An analysis of the data with use of paramagnon models implies that all of the U_6X compounds are strongly-exchange-enhanced paramagnets. Recent Fermi-liquid models are discussed in relation to predictions of p-wave superconductivity, exchange-enhanced paramagnetism, and electron localization in heavy-fermion systems. An empirical correlation is examined between the ratio of the total magnetic susceptibility to the electronic specific heat and the occurrence of either superconductivity or ferromagnetism for a broad class of metallic solids. The correlation suggests that the U_6X compounds are near the boundary between superconducting and ferromagnetic ground states.

Recent studies[1–5] of the low-temperature properties of U_6Fe have revealed that this compound exhibits large values of the electronic coefficient of specific heat $\gamma^* = 155$ mJ/mole K^2 and the initial slope of the superconducting upper critical field $H'_{c2}(T_c) \equiv (dH_{c2}/dT)_{T_c} = -3.4$ T/K. $H_{c2}(T)$ increases linearly below a zero-field superconducting transition temperature $T_c(H=0) = 3.8$ K to $H_{c2} \approx 6.4$ T at $T \approx 2$ K, implying $H_{c2}(T=0) \approx 10$ T. These data are particularly remarkable for a rather low-T_c compound, especially when compared to similar results for high-T_c, high-H_{c2} materials such as A15 and Chevrel phases for which $\gamma^* < 50$ mJ/mole K^2 (Refs. 6 and 7), $-H'_{c2}(T_c) \approx 1.0$–$7.5$ T/K (Refs. 8–10), and $T_c > 10$ K.

Some of the unusual properties of the U_6X (X=Mn, Fe, Co, Ni) compounds were noted earlier with the discovery of the superconductivity of the Mn, Fe, and Co members by Chandrasekhar and Hulm.[11] They pointed out that the trend of T_c with respect to the valence electron concentration e/a deviated from the empirical rules of Matthias for transition-metal superconductors. Hill and Matthias[12] investigated the T_c's of $U_6(X,X')$ alloys and found a regular trend of T_c with e/a which was remarkably similar to the Slater-Pauling correlation between the saturation magnetization of the analogous ferromagnetic (X,X') alloys and e/a. They suggested that this behavior could be evidence for triplet pairing or some type of "magnetic" mechanism for superconductivity in U_6X compounds.

Traditionally, the presence of strong-exchange interactions in highly paramagnetic (or even ferromagnetic) metals have been thought to favor triplet pairing via the exchange of paramagnons (or spin waves in a ferromagnet) between electrons.[12] On the other hand, paramagnons are expected to strongly suppress singlet pairing[13] and lead to weak anomalies in the temperature dependence of the paramagnetic susceptibility.[14,15] Indeed, it is tempting to attribute the relatively low T_c of U_6Fe to the destructive effects of paramagnons, in analogy to the early work of Andres and Jensen[16] for the late transition metals and alloys. In addition, very few superconducting compounds of U or the ferromagnetic $3d$ elements are presently known,[17] whereas the majority of such materials are either normal paramagnets to very low temperatures or exhibit some type of ferromagnetic order.[18] All of these considerations make the low-temperature magnetic behavior of U_6X compounds extremely interesting, and we report here our initial results for the low-temperature magnetization and susceptibility of several U_6X materials. The related question of triplet pairing or magnetic interactions as mechanisms for the superconductivity of these materials is addressed in the discussion section of this paper.

We note that Gordon[19] and Bates and Mallard[20] first performed magnetic measurements on U_6Fe and related compounds at room temperature and a few points above 300 K. These results show that the susceptibilities of all the U_6X compounds (X=Mn, Fe, Co, Ni) increase weakly with temperature between 300 K and their peritectic decomposition temperatures. After our own measurements were completed, we were informed of the low-temperature susceptibility data for U_6Fe obtained earlier by Gann *et al.*[21] Our results for U_6Fe reported below are

©1985 The American Physical Society

in substantial agreement with their data.

We will discuss our results obtained at high and low magnetic field strengths in separate sections. The latter data emphasize metallurgical defects in our samples, and provide an important check of sample quality.

II. EXPERIMENTAL DETAILS

The higher-field magnetization measurements were made with a vibrating sample magnetometer adapted to a 6.0-T, high-homogeneity superconducting magnet. Data were taken at fixed field in the range $4.2 \leq T \leq 280$ K by slowly warming the sample after boiling away the liquid helium in a small insert Dewar surrounding the cryostat. Samples were first cooled to 4.2 K in zero field, and then the field was applied before warming. The magnetization σ at 4.2 K was found to be the same in runs where the sample was either cooled in zero or finite field. Temperatures were measured with a copper Constantan thermocouple located near the sample. Some 4.2-K isotherms were obtained with liquid helium remaining in the cryostat.

Low-field ($H \approx 100$ Oe) and moderate-field ($H \approx 5$ kOe) magnetization measurements were made with a superconducting quantum interference device (SQUID) magnetometer.[22] Samples were routinely 2 mm in diameter and approximately ellipsoidal in shape. The earlier measurements were carried out by rapidly cooling a sample to undetermined low temperatures as it was lowered into the region of the measuring field and finally equilibrated at $T \approx 4.3$ K. Thus, the samples were partially cooled in both zero and finite applied fields. The sample was then measured as it was warmed to a temperature $\lesssim 275$ K and then recooled without changing the applied field.

The large hysteresis observed in the warming and cooling data led us to repeat some of our SQUID magnetometer measurements by first carefully cooling a sample to $T \approx 4.5$ K in a relatively field-free region, and then lowering the sample into the measuring field region. The magnetization was then measured by warming the sample to $T \approx 150$ K, followed by recooling to 4.5 K. Some samples were thermally recycled and measured a second time without removing them from the field region, and these data differed very little from those of the first cooling run. Temperatures higher than 150 K could not be attained in the controlled cooling studies due to well-understood experimental problems.

Almost all of the samples measured were supplied to us by Dr. J. Engelhardt. These materials were carefully characterized in a previous study[23] and the reader is referred to this work for details. An additional $U_{6.1}Fe$ sample (No. II33) was cut from the parent boule used in specific heat (C_P) and H_{c2} measurements reported earlier.[1–3] X-ray analysis of No. II33 was carried out at Los Alamos National Laboratory (LANL) by Dr. B. Roof, and no evidence of any impurity phases could be detected within the sensitivity of the powder technique employed. Metallographic studies of a $U_{6.1}Co$ sample (No. 529) were performed by R. S. Pereyra of LANL, and these results will be discussed below.

All of the sample materials used in this study were melted at a slight U excess (nominal $U_{6.1}X$ stoichiometry), but the terminology U_6X will be used for convenience throughout this paper.

III. HIGH-FIELD RESULTS (U_6Fe AND U_6Co)

Our data for σ versus T for a U_6Fe sample (No. II33) taken at $H=1.0$ T are shown in Fig. 1. σ increases roughly 25% as the temperature is lowered from 300 to 4.2 K. The inset to Fig. 1 shows two isothermal magnetization curves taken at $T=4.2$ and 220 K. A ferromagnetic remanence appears in the 4.2-K curve (a), but the magnetic susceptibilities determined from these curves are identical, i.e., $\chi(4.2\text{ K})=\chi(220\text{ K})=1.55\times10^{-6}$ cm^3/g. The overall magnitude and temperature dependence of σ for this relatively large sample (0.853 g) are in good agreement with the results of Gann *et al.*[21] on a specimen of $U_6Fe_{0.98}$, but their low-temperature values of $\chi \approx (2.00\text{—}2.05)\times10^{-6}$ cm^3/g are in disagreement with the results of Fig. 1. Gordon[19] and Bates and Mallard[20] report room-temperature values $\chi(290\text{ K})=1.97\times10^{-6}$ cm^3/g and 2.04×10^{-6} cm^3/g, respectively. We note that Gordon used powdered samples, whereas Bates and Mallard measured several U-Fe alloy polycrystals containing $\leq$10-at. % Fe, and indirectly deduced a value of χ for U_6Fe.

A smaller piece (0.711 g) of the No. II33 sample boule was measured at $T=4.2$ K and a value of $\chi(4\text{ K})=2.09\times10^{-6}$ cm^3/g was obtained from the high-field data, whereas $\chi(4\text{ K})=2.15\times10^{-6}$ cm^3/g and a remanent moment of 8.85×10^{-3} emu/g were obtained from the lower-field data. Another sample (No. 532, 0.582 g) was also measured, and a high-field $\chi(4.2\text{ K})=2.03\times10^{-6}$ cm^3/g was found, and $\chi(4.2\text{ K})=2.25\times10^{-6}$ cm^3/g with a remanent moment of 5.73×10^{-3} emu/g were extracted from the lower-field data. These results are shown in Fig. 2, and are in excellent agreement with the work of Gor-

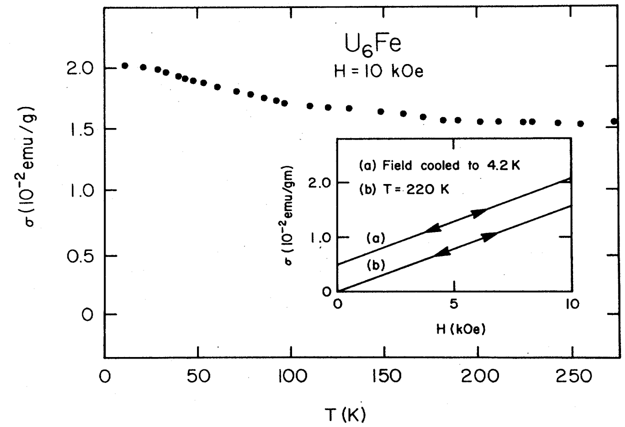

FIG. 1. Magnetization σ vs temperature T for U_6Fe sample No. II33, taken in an applied field $H=1$ T. The inset shows σ vs H for two cases: (a) the sample was cooled from room temperature in the measuring field and then cycled at $T=4.2$ K, and (b) the sample was field cycled at $T=220$ K. The different behavior in curves (a) and (b) is due to the remanent magnetization from the ferromagnetic transition of an impurity phase near 170 K.

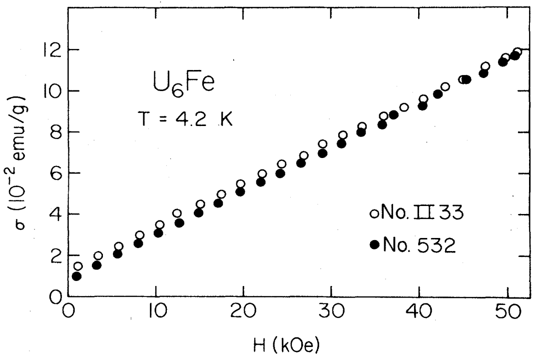

FIG. 2. Magnetization σ vs applied field H for two different samples of U_6Fe. Data were obtained after field cycling the samples at $T=4.2$ K. There are small changes in the slope of σ vs H due to the saturation of small amounts of ferromagnetic impurity phases. Note the discrepancy between the susceptibility values $\chi=d\sigma/dH$ obtained from this plot and those of the inset of Fig. 1.

don, Bates and Mallard, and Gann *et al.*

The relatively small value $\chi(4\ \mathrm{K})=1.55\times10^{-6}$ cm^3/g measured for the 0.853-g piece of U_6Fe No. II33 is difficult to understand as a result of impurity phases. The only evidence we have for sample deterioration under room conditions was observed in Mössbauer effect studies[24] and additional susceptibility data on a 0.0979-g sample of U_6Fe. In the latter case, measurements at 4.2 K and fields up to 4 T yielded $\chi(4\ \mathrm{K})=2.13\times10^{-6}$ cm^3/g, whereas a redetermination made several months later on this piece gave a different value $\chi(4\ \mathrm{K})=2.52\times10^{-6}$ cm^3/g. The Mössbauer measurements on powdered U_6Fe absorbers indicate that after several months storage, a very small satellite peak develops in the ^{57}Fe resonance spectra, presumably due to a slight deterioration of the powdered material.

Another possible explanation of the discrepancies in our susceptibility data is based on neutron diffraction studies of arc-melted and annealed boules,[25] including the piece of No. II33 studied in specific-heat measurements.[1–3] These measurements indicate that very coarse-grained polycrystals can easily by obtained using our sample-preparation procedures. Assuming that the susceptibility of U_6Fe is anisotropic, a significant degree of preferred orientation in our polycrystalline samples could explain the irreproducibility of our χ(4-K) data as well as the consistency between data measured for powdered samples.[19] Further measurements will be necessary to fully explain the magnetic behavior of U_6Fe.

A U_6Co sample was also measured at 4.2 K and $H\leq5$ T, and our results for σ/H versus T at $H=1.2$ and 5.0 T are shown in Fig. 3. The value of $\chi(4\ \mathrm{K})=2.08\times10^{-6}$ cm^3/g obtained from these data are close to the room-temperature value of 1.95×10^{-6} cm^3/g obtained by Gordon.[19] There is clear evidence for a ferromagnetic component in these data with an ordering temperature T_m near 175 K. A small anomaly at 175 K is also present in our U_6Fe data (see Fig. 1), and has also been observed by Gann *et al.*[21] Since we will show that this anomaly is found for all the U_6X materials which have been studied to date, we must assume that it is due to a ferromagnetic U compound common to all members of the U_6X series. In order to estimate the significance of this anomaly, we have assumed that a U impurity phase orders ferromagnetically at ~175 K, and that all of the remanent magnetization observed at 4 K (see Fig. 1) is due to the saturation magnetization of this hypothetical phase. We then assigned a value of 1.2 μ_B per U atom [corresponding to UH_3 (Ref. 26)] as an estimate of the impurity saturation moment and deduced that the mole fraction of U present in a magnetic impurity phase was $\lesssim1\times10^{-4}$ for U_6Co (Fig. 3) and $\lesssim5\times10^{-5}$ (Fig. 1) or $\lesssim5\times10^{-4}$ (Fig. 2) in the case of U_6Fe. These levels of contamination are quite reasonable for the sample-preparation techniques used. The additional temperature dependence of the σ-versus-T data for U_6Fe at $T<175$ K is more difficult to explain, and will be discussed later in this paper.

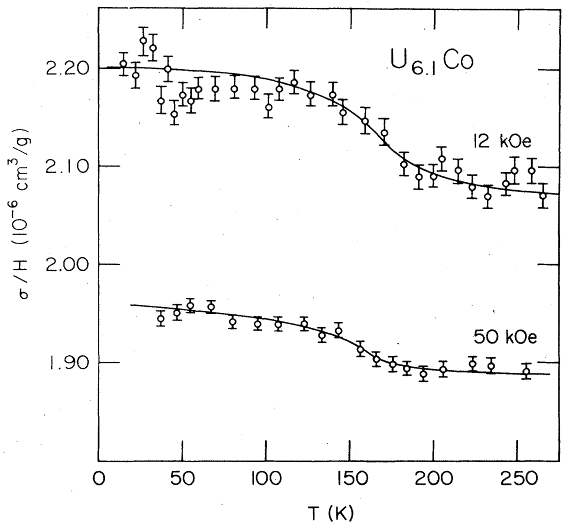

FIG. 3. Magnetization σ divided by applied field H vs temperature T for U_6Co sample No. 529. Data are shown for two different values of constant H. The change in σ/H near 170 K is due to the ferromagnetic transition of a small amount of impurity phase, as corroborated by the field dependence of the data.

IV. LOW-FIELD RESULTS (U_6X AND $U_6Mn_{0.5}Co_{0.5}$)

Lower-field σ/H-versus-T data for two different pieces of an U_6Fe sample (No. 532) are shown in Fig. 4. The anomaly at $T\approx175$ K is made obvious from the thermal hysteresis in the data. It is possible that there is also a rapid change in slope or a kink in the data near 100 K, and this feature is also present in the 10-kOe data of Fig. 1. However, the high-field data of Gann *et al.*[21] exhibit smaller increases in σ below 100 K, and offer no evidence for an intrinsic anomaly below ~150 K. Features in the warming curve data near 20 K in $H=5$ kOe [Fig. 4(b)] should not be taken seriously in view of the measuring procedures employed. Low-field σ/H-versus-T data for two pieces (samples A and B) of a U_6Co sample (No. 529) are shown in Fig. 5. A hysteretic, ferromagnetic behavior appears at $T<200$ K for both samples in agreement with the higher-field data (see Fig. 3). We note that this fer-

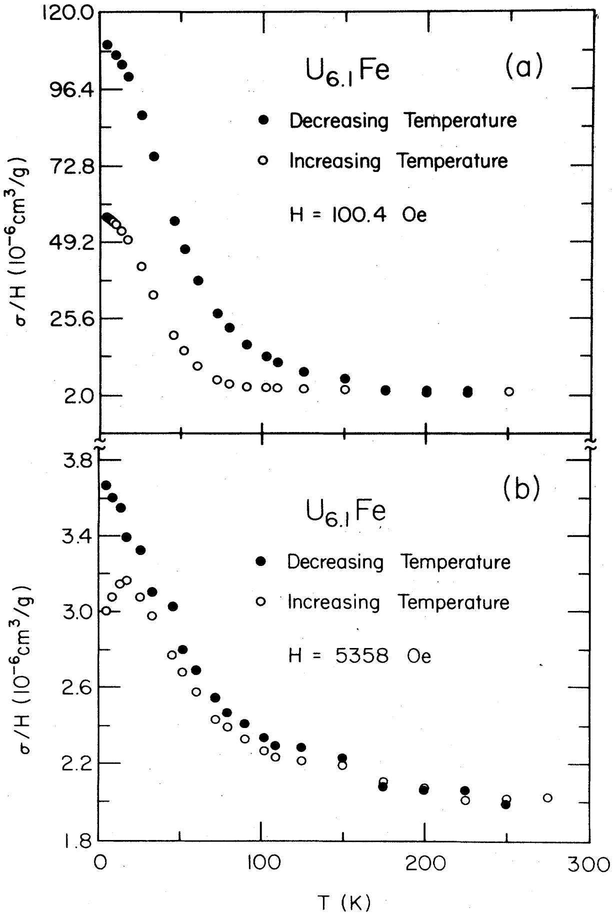

FIG. 4. (a) Magnetization σ divided by applied field $H=10^{-2}$ T for U_6Fe sample No. 532. The samples were initially only partially cooled in the region of applied field (see text for details), and data were first taken by warming from 4 K (open circles), followed by recooling (solid circles) in constant field. The hysteresis is due to the ferromagnetic transition of an impurity phase at $T \approx 170$ K. (b) Magnetization σ divided by applied field $H=0.54$ T for U_6Fe sample No. 532. The measuring conditions and hysteresis effects are similar to those described in (a) above.

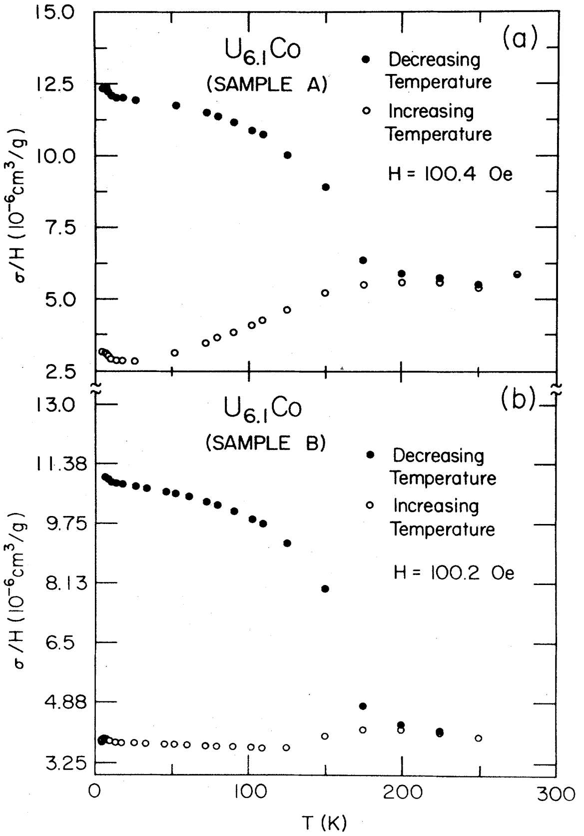

FIG. 5. (a) Magnetization σ divided by applied field $H \approx 100$ Oe vs temperature T for a piece (sample A) of a parent boule of U_6Co sample No. 529. The sample was initially only partially cooled in the region of applied field (see text for details), and data were first taken by warming from 4 K (open circles), followed by recooling (solid circles) in constant field. The hysteresis is due to the ferromagnetic transition of an impurity phase below $T \approx 200$ K. (b) Magnetization σ divided by applied field $H \approx 100$ Oe vs temperature T for a different piece (sample B) of the parent boule of U_6Co sample No. 529. The measuring conditions and hysteresis effects are similar to those described in (a) above.

romagnetic component in our U_6Co samples is approximately 10 times weaker than the analogous component of the U_6Fe data. In addition, the overall character of the hysteresis differs between the U_6Fe and U_6Co measurements.

The differing hysteresis shown in Figs. 4 and 5 led us to remeasure a U_6Co sample by cooling under conditions which were better controlled compared to the experiments depicted in Figs. 4 and 5. The σ/H-versus-T data gathered by either field cooling in 100 Oe or cooling in zero field are shown in Fig. 6. These data suggest that the "intermediate" hysteresis behavior exhibited by U_6Fe in Fig. 4 is a result of rapidly cooling the sample to 4 K by inserting it into the cold bore of an energized superconducting solenoid before warming slowly to take data.

Additional low-field measurements were also performed on samples of U_6Mn (No. 530), U_6Ni (No. 531), and $U_6Mn_{0.5}Co_{0.5}$ (No. 464), and the results for σ/H versus T are shown in Figs. 7 and 8. Some care was taken to first cool the U_6Ni and $U_6Mn_{0.5}Co_{0.5}$ samples in a relatively field-free region.

The σ/H-versus-T behavior of U_6Mn shown in Fig. 7 is quite similar to the U_6Co data of Fig. 5. A ferromagnetic component becomes apparent at $T<175$ K. The U_6Ni and $U_6Mn_{0.5}Co_{0.5}$ data also exhibit ferromagnetic components at somewhat lower temperatures $T \leq 150$ K. We reemphasize that the σ/H data from the 100-Oe measurements of U_6Fe at $T<100$ K shown in Fig. 4 are approximately 10 times larger than *any* of the corresponding data from measurements on the other U_6X samples reported herein. This is not understood at present.

Our low- and high-field magnetic data are summarized in Table I, and are in reasonable agreement with the previous room-temperature susceptibility results of Gordon,[19] with the exception of the rather large σ/H values we have

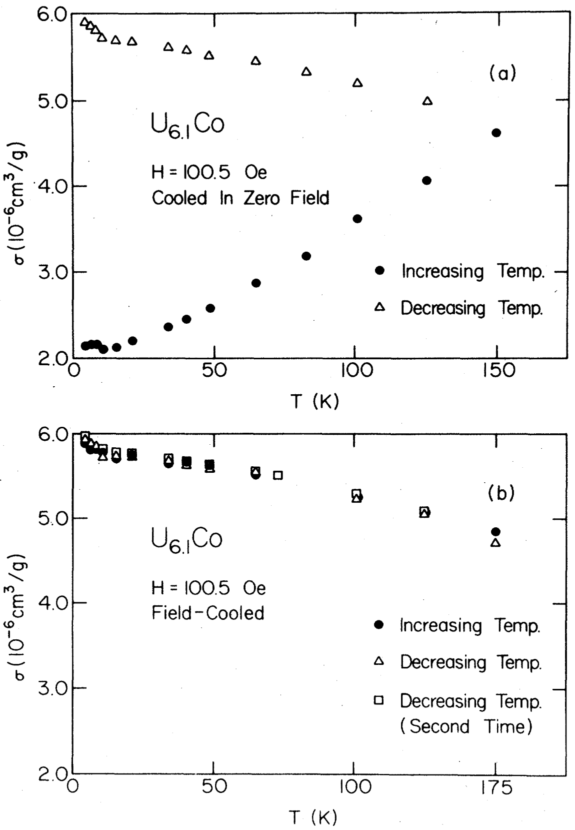

FIG. 6. Magnetization σ vs temperature T in an applied field $H \approx 100$ Oe for a single piece of U_6Co sample No. 529. Data were taken under relatively controlled conditions of field coolings. (a) The sample was initially cooled to 4 K in $H = 0$, then warmed from 4 K in $H = 100.5$ Oe (solid circles), and then recooled without changing H (triangles). (b) The sample was cooled from room temperature to 150 K, and then placed in $H = 100.5$ Oe, followed by additional cooling in constant field to 4 K (triangles). The sample was then warmed (solid circles) and recooled (squares) without changing H. Note these data are identical to those of (a) above for "decreasing temperature." These results verify the presence of a ferromagnetic transition of an impurity phase near 150 K.

observed for our U_6Co samples at low fields. There appears to be a large field dependence to σ/H for U_6Co, even above the ferromagnetic anomaly near 200 K. Further measurements on additional U_6Co samples at higher temperatures will be necessary to investigate this behavior. The irreproducibility of the U_6Fe polycrystal data also deserves further investigation. Recent heat-capacity and critical-field measurements[27] on U_6Fe samples made from particularly high-purity starting materials suggest that the U used in the present study and/or the storage conditions pertinent to the samples supplied to us by J. Engelhardt are not adequate for obtaining optimal superconducting and magnetic data. We have included the results of inductive measurements of the superconducting T_c's of representative samples in Table I in order to aid other workers in assessing the quality of our materials.

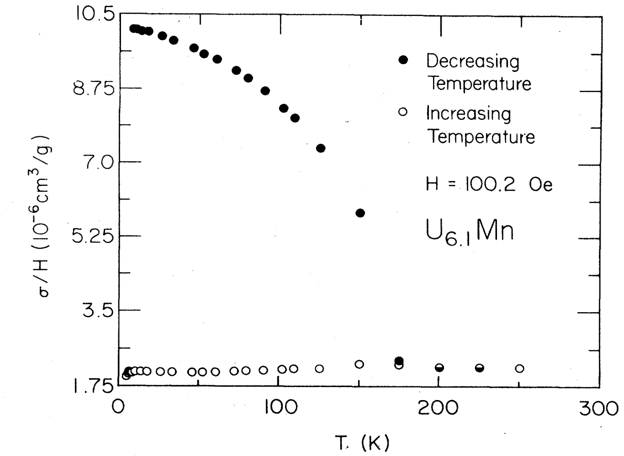

FIG. 7. Magnetization σ divided by constant applied field $H = 100.2$ Oe vs temperature T for a U_6Mn sample No. 530. The sample was initially only partially cooled in the region of applied field (see text for details), and data were first taken by warming from 4 K (open circles), followed by recooling (solid circles) in constant field. The hysteresis is due to the ferromagnetic transition of an impurity phase near $T \approx 175$ K.

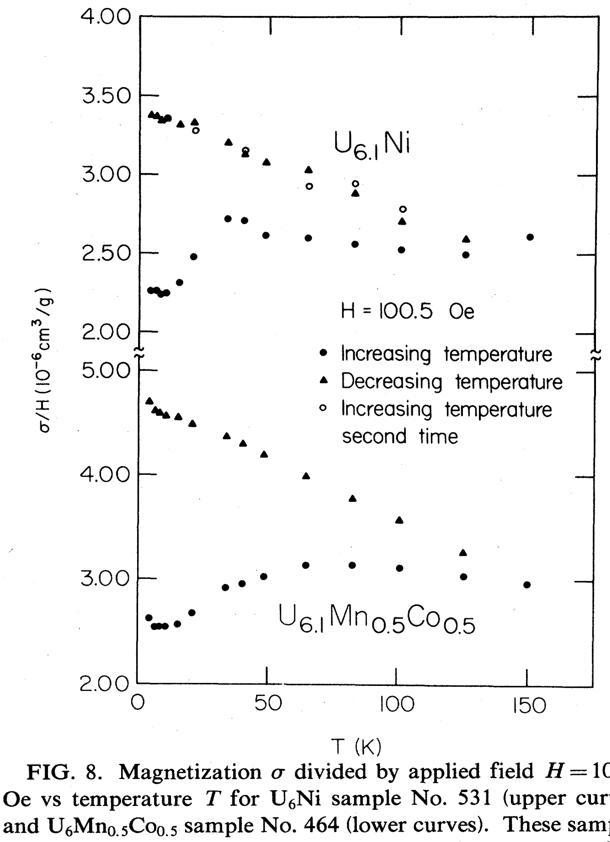

FIG. 8. Magnetization σ divided by applied field $H = 100.5$ Oe vs temperature T for U_6Ni sample No. 531 (upper curves) and $U_6Mn_{0.5}Co_{0.5}$ sample No. 464 (lower curves). These samples were first cooled to 4 K in a field-free region and then the field was applied before warming from 4 K (solid circles). The sample was then recooled (triangles) and rewarmed (open circles) without changing H. The resulting hysteresis is due to the ferromagnetic transition of an impurity at $T \approx 150$ K.

TABLE I. Magnetic and superconducting parameters of sample materials.

Sample	σ/H (10^{-6} cm^3/g)	Measuring temperature (K)	Measuring field (Oe)	T_c(K)[a]	ΔT_c(K)[a]	Remarks
$U_{6.1}Fe$ (No. 532)[b]	2.95	250	100.4	3.79	0.04	See Fig. 4
$U_{6.1}Fe$ (No. 532)[b]	2.03	275	5358			See Fig. 4
$U_{6.1}Fe$ (No. 532)[b]	2.03[c]	4.2	$\leq 5\times 10^4$			See Fig. 2
$U_{6.1}Fe$ (No. 532)[d]	2.13[c]	4.2	$\leq 5\times 10^4$			Early measurement (see text)
$U_{6.1}Fe$ (No. 532)[d]	2.52[c]	4.2	$\leq 5\times 10^4$			Later measurement (see text)
$U_{6.1}Fe$ (No. II33)[b]	2.09[c]	4.2	$\leq 5\times 10^4$	3.76	0.136	See Fig. 2
$U_{6.1}Fe$ (No. II33)[b]	1.55[c]	4.2,220	$\leq 1\times 10^4$			See Fig. 1
$U_{6.1}Co$ (No. 529)[b]	5.86	275	100.4	2.33	0.10	Sample A of Fig. 5
$U_{6.1}Co$ (No. 529)[b]	3.94	250	100.2			Sample B of Fig. 5
$U_{6.1}Co$ (No. 529)[b]	4.61–4.7	150	100.5			See Fig. 6
$U_{6.1}Co$ (No. 529)[d]	2.08[c]	250	$\leq 1.2\times 10^4$			See Fig. 3
$U_{6.1}Co$ (No. 529)[d]	1.90[c]	250	$\leq 5\times 10^4$			See Fig. 3
$U_{6.1}Mn$ (No. 530)	2.21	250	100.2	2.31	0.170	See Fig. 7
$U_{6.1}Ni$ (No. 531)	2.61	150	100.5	0.327[e]	0.013[e]	See Fig. 8
$U_{6.1}Mn_{0.5}Co_{0.5}$ (No. 464)	2.97	150	100.5	2.69[e]	0.06[e]	See Fig. 8

[a] T_c's are representative values for one arbitrary piece of the boule separately measured with an inductive technique. ΔT_c is the measured width (10% to 90% completion) of the transition.

[b] Different pieces of same parent boule.

[c] Corresponds to a susceptibility determined from a magnetization curve taken over the field range cited.

[d] Same pieces of parent boule.

[e] Data taken from Engelhardt (Ref. 23).

V. IMPURITY PHASE CONSIDERATIONS

Virtually all of the magnetization data presented in Figs. 1 through 8 indicate the presence of ferromagnetic remanence at $T \lesssim 175$ K, and occasionally exhibit weaker anomalies near 30 K (see Figs. 1, 3, 4, and 8). We recall that the magnitude of the 175-K anomalies are generally consistent with less than ~ 500 ppm of the U present being tied up in a ferromagnetic phase. Since the presence of such phases can sometimes affect the details of transport, magnetic, and calorimetric data, we have made some attempt to identify potential compounds which could explain the observed anomalies.

We have specifically considered the existing data for the UX_2 compounds ($X=$Mn, Fe, Co, Ni) which are undoubtedly present in our sample materials at small but finite concentrations due to the peritectic formation of the U_6X phases.[28] However, the 175-K anomalies are not easily attributed to the UX_2 compounds since their presence and Curie temperature are essentially independent of the X constituent (unless all of our samples contain appreciable UFe_2 impurity concentrations).

Unfortunately, we do not have chemical analyses available for much of the U metal used in this study, except that it was of 99.9% nominal purity. Such lots of U typically contain small amounts of Ca, Mg, Al, Pb, Si, C, and various $3d$ elements at levels around 1—10 ppm by weight. Further, O and N are common impurities, and the concentration of Fe is generally up to 10 times that of other $3d$ elements. A summary of the magnetic properties of selected U compounds is given in Table II.

Metallographic studies of a $U_{6.1}Co$ (No. 529) sample by R. Pereyra of LANL have been interpreted as evidence for the presence of U oxide present in small inclusions throughout the primary phase grains. A second impurity phase was found to be present in additional inclusions and along grain boundaries. The second phase was tentatively identified as α-U due to its etching behavior and the nature of the U-Fe phase diagram,[19,28] although it is possible that the grain boundary phase is actually composed of two or more cosoluble impurities. These results are in good agreement with the metallurgical results of Gordon and Kaufmann.[28]

Although we cannot rule out the presence of UFe_2 at the 1—10-at. ppm level in our U_6Mn, U_6Co, and U_6Ni samples, it is just as likely that UH_3 or an UN_x phase could be responsible for the 175-K anomaly. It is more certain (given the metallographic results) that features near 30 K are due to any of several UO_x phases, or possibly UPb_3. In any event, the magnetization anomalies near 30 and 175 K appear to be explainable as effects due to reasonable concentrations of ferromagnetic impurities.

TABLE II. Magnetic properties of probable impurity phases in U_6X (f.u. denotes formula unit).

Compound	Magnetic behavior[a]	Effective moment (μ_B/f.u.)	Ordering temperature (K)	Ordered moment (μ_B/f.u.)	References[b]
UMn_2	(structural transition at 212 K)	6.6	<4		89
UFe_2	FM	2.0	147—172	1.0	
UCo_2	P		<1.1		
UNi_2	FM		21	0.04	90
UO_2	AFM	3.2	30.8	1.8	90
UO_x	(various)		<30		
UN	AFM	3.1	52	0.75	
α-U_2N_3	AFM	3.8	96		
β-U_2N_3	FM	2.9—3.7	182—235		
α-UH_3	FM	2.8	178	<0.9	
β-UH_3	FM	2.5	168—181	1.2	
UC	P		<5		
U_2C_3	P	3.6	<4		
UC_2	P		<80		
U_3Si	TIP		<85		
U_3Si_2	P		<85		
U_3Si_5	P	10.2	<4		
$USi_{1.88}$	P		<1.3		
USi_3	P		<4		
UAl_2	P		<0.08		91
UAl_3	P		<40		
UPb_3	AFM	3.2	32	1.6	92
UCu_5	AFM		15		93

[a] P denotes paramagnetic, TIP denotes temperature-independent paramagnetism, FM denotes ferromagnetic, and AFM denotes antiferromagnetic.

[b] Data taken from Ref. 18, unless otherwise stated.

TABLE III. Structural and superconducting properties of U_6X compounds. (Except where noted, data were taken from Ref. 30.)

Compound	Lattice parameters (Å)[a] a	c	Molar volume per f.u. (cm^3)	γ^* (10^4 erg/cm^3 K^2)	$\omega_{\log}$ (K)	T_c (K) (calorimetric)	$\frac{\Delta C}{\gamma^* T_c}$
U_6Mn	10.312	5.255	84.168	1.17	92.4	2.21	1.6
U_6Fe	10.303	5.235	83.706	1.87	83.4	3.70	2.1
U_6Co	10.323	5.191	83.321	1.58	91.2	2.29	1.7
U_6Ni	10.390	5.156	83.839	1.09	100	0.33[b]	

[a] Data taken from Ref. 23.

[b] Estimated.

VI. ANALYSIS

Since we have not yet completed detailed magnetization curves for temperatures $4\ K < T < 300\ K$, there may be small features in the temperature dependence of $\chi(T)$ which remain to be resolved, but the data of Gann *et al.* for U_6Fe (Ref. 21) suggest that this is unlikely. However, we do have some evidence (see Figs. 1 and 4) that the behavior of U_6Fe is peculiar below $T \approx 100$ K, in that the magnitude and temperature dependence of σ/H of the Fe compound are somewhat greater than those of the other U_6X materials. Of course, this could be due to the presence of impurity phases. On the other hand, recent Mössbauer studies[24,29] have revealed anomalies near 100 K in the temperature dependence of the recoil-free fraction and the isomer shift. It would therefore be of interest to obtain additional magnetization curves near 100 K for very-high-purity U_6Fe samples or single crystals. However, in the analysis which follows we will neglect the possibility of small features in $\chi(T)$ deriving from potential phase transitions or "Fermi-liquid effects,"[14,15] and we shall assume that the room-temperature susceptibility and magnetization measurements are good approximations to the low-temperature χ in cases where magnetization curves taken at ~4 K are not yet available.

A. Effective mass

The exceptionally large values of γ^* found for the U_6X compounds[30] suggest that the magnetic properties of these materials may be renormalized by strong interactions between band electrons. Such interactions can lead to a sizeable enhancement of the electronic effective mass m^* within an isotropic Fermi-liquid model:

$$m^* = \frac{3\hbar^2\gamma^*}{k_B^2}\left[\frac{\Omega}{3\pi^2 Z}\right]^{1/3} . \tag{1}$$

Here, Ω denotes volume per atom and Z denotes number of interacting fermions per atom. We have summarized relevant structural and specific-heat data for the U_6X compounds in Table III.

It is important to note that the γ^* values quoted in Table III are constrained by entropy arguments and are considered to be rather accurate.[30] (The γ^* value for U_6Ni listed in Table III was not constrained by entropy conditions due to the low T_c of this compound. However, the quoted γ^* was found to be independent of the several methods of analysis used to determine it in Ref. 30.) Therefore, the uncertainty in m^* depends only on the accuracy of Z and, more importantly, the applicability of an isotropic Fermi-liquid model to U_6X. Such a model is widely applied in discussions of "heavy-fermion" superconductors, and is a useful framework for comparing data for various materials.[31] Our results for m^*/m_e (m_e denotes free-electron mass) are collected in Table IV. Note that although a very wide range of $0.25 < Z \leq 6$ has been used, it is clear that all of the U_6X compounds exhibit unusually high effective masses for any reasonable choice of Z. In lieu of x-ray spectroscopic data and band-structure calculations, we expect $Z \approx 3 \pm 1$ for both the U- and X-element constituents. Values of $Z \approx 2 \pm 1$ have been advanced for $CeCu_2Si_2$ (Ref. 32) and UBe_{13} (Refs. 33—35), but these latter compounds exhibit behavior which suggests that their f states may be less hybridized with band states in comparison to U_6X. Further, recent Fermi-liquid-model calculations[36,37] yield

TABLE IV. Thermal effective masses of U_6X compounds. (Values of m^*/m are deduced from the γ^* data of Ref. 30.)

Z	$(m^*/m_e)U_6Mn$ ($\Omega = 1.9957 \times 10^{-23}$ cm^3)	$(m^*/m_e)U_6Fe$ ($\Omega = 1.9847 \times 10^{-23}$ cm^3)	$(m^*/m_e)U_6Co$ ($\Omega = 1.9756 \times 10^{-23}$ cm^3)	$(m^*/m_e)U_6Ni$ ($\Omega = 1.9879 \times 10^{-23}$ cm^3)
0.25	31.4	50.0	42.1	29.2
0.50	24.9	39.7	33.4	23.2
1.00	19.8	31.5	26.5	18.4
1.50	17.3	27.5	23.2	16.1
2.00	15.7	25.0	21.07	14.6
3.00	13.7	21.8	18.4	12.8
4.00	12.5	19.9	16.7	11.6
5.00	11.6	18.4	15.5	10.8
6.00	10.9	17.3	14.6	10.1

$m^*/m_e \approx 22$ in the case of U_6Fe, consistent with our estimate of $Z \approx 3$.

B. Paramagnon model

We will analyze our susceptibility results using the decomposition

$$\chi(T) = \chi_d + \chi_0^* + \chi_P^* , \tag{2}$$

where χ_d is the core diamagnetic term, χ_0^* is the orbital contribution, and χ_P^* is the Pauli spin susceptibility. The asterisks emphasize the fact that χ_0^* and χ_P^* are expected to be significantly renormalized by strong interactions in high effective-mass materials.

More specifically, the relatively frequent occurrence of large γ^* values and strong paramagnetism among light actinide materials is believed to be a consequence of the semilocalized nature of the $5f$-electron states at the beginning of the actinide series.[38] Certain anomalous thermal properties of these materials can then be (somewhat naively) attributed to the presence of narrow, $5f$-derived features in the renormalized density of states at the Fermi energy $N^*(E_F) \sim N(E_F) m^*/m_e$, where $N(E_F)$ is the "bare" density of states appropriate to the electron system in the absence of the interactions which lead to $m^*/m_e > 1$. Assuming the quasilocal $5f$-electron states also experience strong-exchange interactions, a large $N^*(E_F)$ would imply that the paramagnetic spin susceptibility would be exchange enhanced according to the relation[39]

$$\chi_P^* = \chi_P \mathcal{S} = \chi_P (1-\bar{I})^{-1} = \chi_P [1 - I N(E_F)]^{-1} , \tag{3}$$

where I is the exchange interaction strength.

The orbital term in Eq. (2) is rather simple in the case of an isotropic electron liquid:[40]

$$\chi_0^* = -\frac{1}{3} \left[\frac{m_e}{m^*} \right]^2 \chi_P^* . \tag{4}$$

However, this diamagnetic form is only appropriate to a single band, and in the case of actinide materials, large paramagnetic contributions to χ_0^* are expected[41] from "narrow" [high $N(E_F)$] d- and f-derived bands. Further, recent calculations[42,43] have demonstrated that the anticipated strong spin-orbit coupling in actinides will also complicate the form of χ_0^*. We are therefore forced to assume that $0 \le \chi_0^* \le 2\chi_P^*$, since the Landau-Peierls diamagnetic contribution given in Eq. (4) is evidently negligible in high-mass materials. The validity of our assumptions will be discussed in more depth later in this paper.

The core diamagnetism χ_d can be estimated from tabulated values[44] for U^{6+} and the highest quoted valence state of the X component of U_6X. These contributions are small compared to χ_P^*, as shown in Table V, and are not critical in our analysis.

We will follow a method of analysis recently outlined by Orlando and Beasley,[45] based on the earlier work of Jensen and Andres[16] and Allen and Dynes.[46] The effects of the screened Coulomb, electron-phonon, and exchange interactions on T_c are modeled with the following equation:

$$T_c = \frac{\omega_{\log}}{1.2} \exp \left[\frac{1+\lambda+\lambda_s}{\mu^* + \lambda_s - \lambda} \right] . \tag{5}$$

$\omega_{\log}$ can be obtained from the specific-heat results and analyses of Ref. 30, and μ^*, λ, and λ_s parametrize the strengths of the three respective interactions listed above. λ_s can be related to the susceptibility enhancement of Eq. (3) via[39,45,47]

$$\lambda_s = \frac{9}{2} \frac{\mathcal{S}-1}{\mathcal{S}} \ln \left[1 + \frac{\bar{P}_1^2}{12} (\mathcal{S}-1) \right] . \tag{6}$$

Here, $\bar{P}_1$ is a normalized (with respect to the Fermi wave vector) momentum cutoff for the paramagnon interaction I, and it is usually supposed that $\bar{P}_1 \approx 0.5$—2.0.[39] The mass enhancement is then given by

$$m^*/m_e = 1 + \lambda + \lambda_s , \tag{7}$$

and the susceptibility and specific heat are related by

$$\frac{\gamma^*}{\chi_P^*} = \frac{1}{3} \left[\frac{\pi k_B}{\mu_B} \right]^2 (1+\lambda+\lambda_s) \mathcal{S}^{-1} . \tag{8}$$

Equations (1)—(3) and (5)—(8) can be solved simultaneously to provide values of λ_s and $\mathcal{S}$ appropriate to the U_6X compounds. Specifically, Eqs. (5) and (8) can be solved to eliminate λ and the resulting equation for λ_s in terms of $\mathcal{S}$ can be graphically compared to Eq. (6). Several of the input parameters of the analysis must be estimated. Accordingly, we have allowed for as wide a range of "unknown" variables as seemed physically reasonable, and set $0 \le \chi_0^* \le 2\chi_P^*$ [Eq. (2)], $0.5 \le \bar{P}_1^2 \le 3.0$ [Eq. (6)], $0.25 \le Z \le 6$ [Eq. (1)], and $0.1 \le \mu^* \le 0.2$ [Eq. (5)]. The results of this procedure are shown in Figs. 9 and 10, and important parameters are summarized in Table VI. We emphasize that Eq. (8) assumes a free-

TABLE V. Magnetic susceptibility data for U_6X compounds.

Compound	$\chi(4\ \text{K})$ (10^{-3} cm^3/mole)	χ_d (10^{-4} cm^3/mole)	χ_P^* ($\chi_0^*=0$) (10^{-3} cm^3/mole)	χ_P^* ($\chi_0^*=\chi_P^*$) (10^{-3} cm^3/mole)	χ_P^* ($\chi_0^*=2\chi_P^*$) (10^{-3} cm^3/mole)
U_6Mn	3.1[a]	−1.185	3.2	1.6	1.1
U_6Fe	3.0	−1.190	3.1	1.5	1.0
U_6Co	2.8[a]	−1.193	2.95	1.5	0.98
U_6Ni	3.0[a]	−1.195	3.1	1.55	1.0

[a] Estimated from room-temperature data of Ref. 19 and results reported herein.

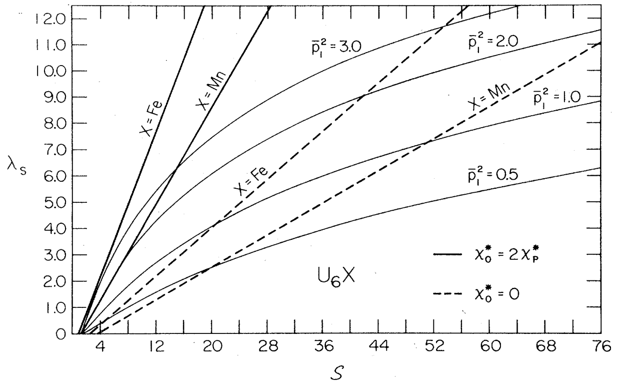

FIG. 9. Paramagnon interaction parameter λ_s vs Stoner exchange-enhancement parameter $\mathcal{S}$ for U_6X ($X=$Fe, Mn) compounds. The curves shown represent a graphical solution of Eqs. (6) and (8) of the text. The thin curves are plots of Eq. (6) for four potential values of the paramagnon interaction cutoff $\bar{P}_1^2$, and the thick straight lines are plots of Eq. (8) for different ratios of the orbital (χ_o^*) and Pauli spin (χ_P^*) susceptibilities, corrected according to Eq. (2) (see text for details). The region of allowed values of ($\mathcal{S}$, λ_s) is bounded by the appropriate solid and dashed straight lines for each element X and the $\bar{P}_1^2=0.5$ and 3.0 curves.

electron g factor of 2 and thereby neglects spin-orbit coupling.[43]

It is interesting to note that all of the U_6X compounds have $8 \leq \mathcal{S} \leq 70$ (depending on the choices of $\bar{P}_1^2$ and χ_0^*) and very large values of λ and λ_s, mainly due to the large γ^* and χ values measured for these materials. Of course, one might suppose that $m^*=m_b(1+\lambda+\lambda_s)$, where m_b is the band mass obtained from the lattice potential without electron-phonon or paramagnon renormalizations. The λ and λ_s values could then be reduced several fold in the case of very narrow f or f-d hybrid bands. However, such considerations are beyond the scope of the simplified models discussed here. We can only conclude that within an elementary paramagnon approach, all of the U_6X compounds appear to be strongly-exchange-enhanced paramagnets.

Although further experimental and theoretical work will be necessary to refine the estimates of λ, λ_s, and $\mathcal{S}$ presented in Table VI, the available data for the superconducting upper critical field (H_{c2}) provide a useful check of our paramagnon analysis. For example, H_{c2} cannot exceed the "Pauli paramagnetic limit" $H_P(T=0)$, which is estimated (in the absence of spin-orbit scattering) via the following relation:[45]

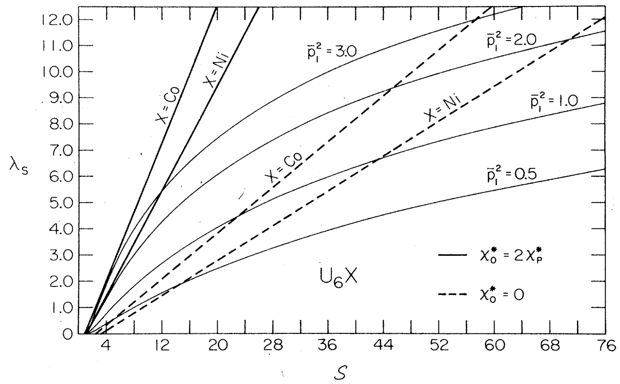

FIG. 10. Paramagnon interaction parameter λ_s vs Stoner exchange-enhancement parameter $\mathcal{S}$ for U_6X ($X=$Co, Ni) compounds. The curves shown represent a graphical solution of Eqs. (6) and (8) of the text. The thin curves are plots of Eq. (6) for four potential values of the paramagnon interaction cutoff $\bar{P}_1^2$, and the thick straight lines are plots of Eq. (8) for different ratios of the orbital (χ_o^*) and Pauli spin (χ_P^*) susceptibilities, corrected according to Eq. (2) (see text for details). The region of allowed values of ($\mathcal{S}$,λ_s) is bounded by the appropriate solid and dashed straight lines for each element X and the $\bar{P}_1^2=0.5$ and 3.0 curves.

$$H_P(0)=(1.86\ \mathrm{T/K})T_c(1+\lambda+\lambda_s)\mathcal{S}^{-1}$$
$$=(2.55\times10^{-5}\ \mathrm{K/Oe})\frac{\gamma^*}{\chi_P^*}T_c\ . \qquad (9)$$

Using the U_6Fe data of Tables III and V, we find 4.8 T$\leq H_P(0) \leq 14.8$ T. Recent measurements[48] on U_6Fe demonstrate that $H_{c2} \geq 10$ T for $T \leq 0.5$ K, implying $\chi_0^* \geq \chi_P^*$, neglecting spin-orbit scattering.

On the other hand, if we neglect Pauli limiting, we can estimate the maximum upper critical field $H_{c2}^*(T=0)$:[45]

$$H_{c2}^*(0)=-0.693T_cH_{c2}'(T_c)\ . \qquad (10)$$

Using $H_{c2}'(T_c)=-3.42$ T/K (Refs. 1–3) and the inductively determined $T_c(H=0)\approx3.80$ K, we find $H_{c2}^*(0)\approx9.0$ T, a value already well exceeded by the data for $T \leq 1.0$ K.[48] Therefore, traditional models[49,50] of the upper critical field are not in quantitative agreement with these data, despite the use of the improved renormalization procedures of Orlando and Beasley.[45] We are therefore reluctant to draw any further conclusions concerning the renormalization parameters λ, λ_s, or $\mathcal{S}$.

TABLE VI. Summary of paramagnon parameters for U_6X compounds.

Compound	m^*/m_e	λ	λ_s	$\mathcal{S}$	μ^{*a}	$\bar{P}_1^2$
U_6Mn	11–31	6.5–19.3	3.5–10.7	8.5–74	0.13	(see Figs. 9 and 10)[b]
U_6Fe	17–50	11–33	5–16	8–72	0.13	(see Figs. 9 and 10)[b]
U_6Co	15–42	9.2–26.6	4.8–14.4	8–68.5	0.13	(see Figs. 9 and 10)[b]
U_6Ni	10–29	5.4–17.5	3.6–11.5	8–71	0.13	(see Figs. 9 and 10)[b]

[a] The use of values $0.1 \leq \mu^* \leq 0.2$ does not strongly affect the results for the other parameters listed.

[b] Note that $\bar{P}_1^2$ enters the analysis only through Eq. (6) and the corresponding curves drawn in the graphical solution shown in Figs. 9 and 10; the results are seen to be consistent with a wide choice of $\bar{P}_1^2$. However, if one restricts $\bar{P}_1^2 \leq 3.0$, the upper limits given here for $\mathcal{S}$ and λ_s will be reduced according to Figs. 9 and 10.

C. Landau Fermi-liquid analysis

The paramagnon model has been extensively applied to analyses of the physical properties of liquid ^{3}He (Refs. 39, 47, and 51) and has been particularly useful in understanding the triplet-paired superfluid states.[51] However, the model has had mixed success in quantitatively accounting for various thermal and transport data.[39,47,51] In particular, a simultaneous fit of the magnetic susceptibility and specific-heat measurements was found to be problematic.[51,52] Nevertheless, a more complete treatment of both density (not included in the basic paramagnon theories) and spin fluctuations within a Landau Fermi-liquid approach yielded an improved comparison between theory and experiment in the case of ^{3}He (Refs. 52–54).

It has been pointed out that the paramagnon and Landau approaches differ in their renormalizations of the static magnetic susceptibility.[52] Specifically, the Landau renormalization is written

$$\chi_P^* = \frac{(m^*/m_e)\chi_P}{1+F_0^a} , \tag{11}$$

where χ_P is the free-Fermi-gas spin susceptibility and F_0^a is the $l=0$ member of the set of antisymmetric Landau parameters F_l^a.[55] On the other hand, the paramagnon model does not explicitly consider the electron-phonon interaction or band-structure effects, and is frequently applied under the assumption that $\underset{\sim}{I} \leq 1$, so that the exchange-enhancement effects and paramagnon renormalization of m^* are expected to dominate the physical properties of interest. Accordingly, it has been generally assumed that the paramagnon renormalization of χ_P^* given in Eq. (3) does not explicitly depend on the effective mass[51,56] or the electron-phonon interaction relevant to the case of metals.[57] However, Levin and Valls[51] have argued that this distinction is artificial, at least in the limit $\underset{\sim}{I} \rightarrow 1$, where the Fermi liquid is near a ferromagnetic instability.

In contrast, the phenomenological approach of Landau includes *all* interactions involving the fermions. Problems therefore arise when particular (and incomplete) microscopic models are adopted to calculate the Landau parameters. We are not aware of any "practical," microscopic model which can be used to fit experimental data including, self-consistently, the effects of paramagnons, phonons, and a crystal potential, although treatments of the superconducting transition temperature of such a system have appeared.[13,16]

The Landau model is frequently compared to experiment by analyzing various ratios of measurable quantities in order to obtain a self-consistent set of Landau parameters which describe the fermion interactions. For example, in the case of an isotropic Fermi liquid we can express the Landau parameter F_0^a in terms of the experimental ratio $\mathscr{R}_0$, where

$$\mathscr{R}_0 \equiv \frac{1}{3}\left[\frac{\pi k_B}{\mu_B}\right]^2 \frac{\chi_P^*}{\gamma^*} = (1+F_0^a)^{-1} \tag{12}$$

and we have assumed the renormalization of Eqs. (1) and (11).

Unfortunately, it is not usually clear how to extract the appropriate value of χ_P^* from data for a real metallic system where band-structure effects, spin-orbit coupling, and the degree of electron localization complicate the decomposition of the experimental $\chi(T)$ into various contributions [see Eq. (2)]. For example, the localized impurity state contributions to $\chi(T)$ and the specific heat $C(T)$ of "model" (spin-$\frac{1}{2}$) Kondo alloys have been analyzed within a Fermi-liquid approach[58,59] which defines the "Wilson ratio" $\mathscr{R}_W$:

$$\mathscr{R}_W \equiv \lim_{T/T_K \rightarrow 0} \left[T \frac{\chi_i(T)}{C_i(T)} \right] , \tag{13}$$

where $\chi_i(T)$ and $C_i(T)$ implicitly refer to only the Kondo impurity contributions to $\chi(T)$ and $C(T)$ of the alloy.

These results have been generalized to more realistic expressions which take into account the orbital angular momentum and strong spin-orbit coupling appropriate to rare-earth Kondo alloys or intermediate valence compounds, and it has been argued[60,61] that [Note that Wilson's original expression for $\mathscr{R}_W(\approx 2$ for $T \ll T_K)$ sets $g, \mu_B \equiv 1$ (Ref. 59).]

$$\mathscr{R}_W = \frac{\chi_{\rm CW}^*}{J(J+1)\gamma^*} \left[\frac{\pi k_B}{g\mu_B}\right]^2 , \tag{14}$$

where g is the g factor, $\mathbf{J}$ is the total angular momentum of the $4f$ state, and $\chi_{\rm CW}^*$ is the Curie-Weiss contribution to χ for $T \ll T_0$ (T_0 is either the Kondo temperature T_K or the valence fluctuation temperature). We emphasize that in practice, one must know how to extract $\chi_{\rm CW}^*$ from $\chi(T)$ in the presence of finite non-$4f$ contributions to $\chi(T)$, and to account for the noninclusion of phonon interactions in γ^* in Eq. (14). It is therefore usually necessary to assume that at $T \ll T_0$, the $4f$ contributions dominate χ and C.

Nevertheless, Batlogg *et al.*[62] have noted that $CeCu_2Si_2$ samples show a strong correlation between estimated values of $\mathscr{R}_W$ and the presence of superconductivity at $T_c \leq 1$ K. It is therefore interesting to extend such a correlation to the U_6X compounds. However, it is extremely difficult to assign values of J and g to U ions since the crystalline electric field and spin-orbit splittings of the $5f$ states are comparable, and the $5f$ wave functions are expected to be significantly delocalized compared to the $4f$ Kondo case appropriate to Eq. (14). (Note that none of the U_6X compounds exhibit Curie-Weiss behavior at any temperature.) Despite the many ambiguities in deriving values of $\mathscr{R}_W$ from experimental data, Stewart[31] has noted that among "heavy-fermion" materials where $\gamma^* \geq 400$ mJ/mole K^2, the possible values of $\mathscr{R}_W$ appear to correlate with the presence or absence of superconductivity and ferromagnetism. The materials which Stewart reviewed are relatively simple to analyze in that χ and γ^* are probably completely dominated by contributions from the heavy-fermion quasiparticles.

We prefer to compare our results for the U_6X compounds to a larger group of "narrow-band" materials and define a figure of merit which is directly accessible from experiment without making ambiguous corrections. We have therefore adopted a tentative measure of the degree

TABLE VII. Experimental values for the enhancement ratio of high-γ^* compounds and selected elements.

Compound	$\langle d \rangle^a$ (Å)	χ^b (10^{-3} cm^3/mole)	γ^b (mJ/mole K^2)	$\mathscr{R}$	$T_c{}^b$ (K)	References
U_6Mn	~3.2	3.06	98.8	2.25	2.21	This work, 19 and 30
U_6Fe	~3.2	3.1	156.8	1.4	3.7	This work, 19, and 30
U_6Co	~3.2	3.0	131.7	1.6	2.29	This work, 19, and 30
U_6Ni	~3.2	3.0	91.7	2.25	~0.33	This work, 19, and 30
α-U	~3.1	0.37	12.2	~2.2	≤2.1	18 and 94–97
U_2PtC_2	3.52	4.4	150	2.1	1.47	88
UPt_3	4.12	7.0	450	1.1	0.54	66 and 98
$NpBe_{13}$	5.13	51	1700	2.2	3.8 (AFM)	99
$PuBe_{13}$	5.15	17.5	225–600	2.1–5.7		99
UBe_{13}	5.13	15.0	1100	0.99	0.86	35
U_2Zn_{17}	4.39	25	1070	1.7	9.7 (AFM)	64
UCd_{11}	6.56	38	840	3.3	5.0 (AFM)	100
UPt_5	5.25	2.7	85	2.3		65 and 98
UPt_2	3.81	4.0	77	3.8		65 and 98
USn_3	4.63	9.52	169	4.1		101 and 102
UAl_2	3.38	4.34	143	2.2		103
$CeRu_2$	3.26	0.86	40.8	1.5	6.2	104 and 105
α-Ce (1 bar)	3.27	0.66	12.8	3.75		106 and 107
α-Ce (11 kbar)		~0.51	11.3	3.3		108 and 109
α-Ce (50 kbar)				~3.2^c	~5×10^{-2}	110
$CeCu_2Si_2^d$	4.1				<1	111
$CeRu_3Si_2$		0.94	39	1.8	1.25	112
$CeAl_3$	4.43	36	1620	1.6		113
$CeCu_6$	4.83	27	1550	1.3		114–116
$CeBe_{13}$	5.17	8.1	115	5.1		117 and 118
$CeSn_3$	4.72	3.0	75	2.9		118 and 119
$CePd_3$	4.13	1.4	55	1.85		120
$CeRh_3$	4.02	0.97	14	5.05		120 and 121
Ir	2.29	0.02	3.27	0.45	0.11	16 and 22
Rh	2.27	0.092	4.65	1.45	3.25×10^{-4}	122–124
Pt	2.34	0.208	6.41	2.4		87 and 122
Pd	2.32	0.717	9.42	5.55	$<8\times10^{-5}$	67, 87 and 125

[a] $\langle d \rangle$ equals the average of the shortest U-U or Ce-Ce distances ("Hill distance") or nearest-neighbor distance. Structural data were taken from Refs. 126 and 127 or other quoted references.

[b] Values of χ and γ^* are actually taken from data at $T \geq T_c$ instead of $T \to 0$ [see Eq. (15)] in the case of superconductors and ferromagnets. Antiferromagnetic transitions are denoted as AFM.

[c] Extrapolated.

[d] Magnetic and colorimetric data are sample dependent: see Refs. 62 and 31.

of "magnetic enhancement" exhibited by a material via the limiting value of the *uncorrected experimental ratio* $\mathscr{R}$ (the limit at $T=0$ is strictly enforced only in the case of *normal* Fermi liquids which do not undergo superconducting or ferromagnetic transitions at accessible temperatures; in these latter cases, we will evaluate $\mathscr{R}$ at temperatures $T \gtrsim T_c$ in order to ascertain the limits of stability of the normal state, as defined by $\mathscr{R}$):

$$\mathscr{R} \equiv \lim_{T\to 0} \frac{\chi^T}{3C} \left[\frac{\pi k_B}{\mu_B} \right]^2 . \qquad (15)$$

Note that we do not attempt to separate various effects due to spin-orbit coupling, orbital paramagnetism, electron-phonon coupling, etc. In the approximation of an isotropic, spin-$\frac{1}{2}$ electron gas with no orbital susceptibility, $\mathscr{R} \to \mathscr{R}_0 \equiv (1+F_0^a)^{-1}$. On the other hand, the definition of $\mathscr{R}$ is completely consistent with the Landau approach for a "real metal" in that all fermion interactions can in principle be included in this parametrization of experimental data. The *key question* is to what degree is the value of $\mathscr{R}$ related to the "exchange enhancement" of the fermion susceptibility or the occurrence of either superconductivity or ferromagnetism?

We have summarized some of the available data and resulting values of $\mathscr{R}$ for narrow-band or heavy-fermion materials in Table VII. There appear to be general trends linking $\mathscr{R}$ with the occurrence of superconductivity or ferromagnetism in the surveyed systems. First, nearly all the superconductors listed exhibit values of $\mathscr{R} \lesssim 2.0$, whereas the nonsuperconductors (including ferromagnets) have $\mathscr{R} \gtrsim 2.0$. Second, within a closely allied group of materials such as the U_6X compounds, the $M\text{Be}_{13}$ materials, or the transition elements Ir, Rh, Pt, and Pd, the value of the superconducting T_c inversely correlates with $\mathscr{R}$.

However, a number of exceptions to the general trends cited seem to occur in the cases of $CeAl_3$, $CeCu_6$, U_2Zn_{17}, U_6Mn, U_6Ni, α-U, and α-Ce. Most of these "anomalies" can be accounted for. The α-Ce and α-U data were obtained at high pressures (α-U data are extremely sensitive to the stability of the charge-density-wave state at ambient pressures[63]), and are therefore subject to substantial experimental inaccuracies or extrapolations. The $\mathscr{R}$ value of U_2Zn_{17} is subject to ambiguities involved in determining the lattice specific heat by using data for the Th_2Zn_{17} analog.[64] Such a procedure has been found to be quantitatively inadequate, for example, in the case of UPt.[65] The rather low $\mathscr{R}$ values for the (so-far) nonsuperconducting compounds $CeAl_3$ and $CeCu_6$ are more difficult to understand. However, there is definite evidence that the heavy-fermion superconductors can be extremely sensitive to defects and strain.[31,66] These two compounds may well be excellent candidates for superconductivity if sufficiently ideal samples can be made (Stewart[31] has also speculated that $CeCu_6$ exhibits a value of $\mathscr{R}_W$ which is sufficiently low to suggest a superconducting ground state).

It is worth emphasizing that these correlations also appear to hold for the noble transition elements, a fact which has an important implication. The $\mathscr{R}$ ratio deduced for Pd suggests that this archtypical paramagnon solid is a very poor candidate for superconductivity, as is Pt to a lesser degree. This prognosis is consistent with the most recent experimental results to ultralow temperatures,[67] but assumes that the pairing interactions relevant to Pd are comparable to cases listed in Table VII.

The superconducting T_c's of the U_6X compounds roughly correlate with $\mathscr{R}$ and are consistent the general trend that T_c is rapidly suppressed near $R \sim 2$. However, the rather large value $\mathscr{R}=2.25$ deduced for U_6Mn and U_6Ni can also be viewed as anomalous in the context of Table VII. The relatively modest magnitude of $\gamma^* \sim 100$ mJ/mole K^2 observed for these compounds suggests that orbital paramagnetism may be competitive with the Pauli contribution and that these two terms must be separated in an analysis of magnetic enhancement effects on superconductivity. We know of no calculation which yields the Van Vleck paramagnetism within a Fermi-liquid approach; it would be very useful to know the dependence of this contribution on m^*/m_e, in analogy to Eq. (4). We have not considered the traditional Van Vleck contribution of the form appropriate to a localized state of total angular momentum **J** since the $5f$ states are probably delocalized in the U_6X compounds. If χ_0^* can be neglected compared to χ_P^*, then U_6Mn and U_6Ni would appear to be very strongly-exchange-enhanced superconductors, based on Eq. (3) and the trends of Table VII.

We have attempted to gauge the reliability of the correlation between $\mathscr{R}$ and the nature of the low-temperature ground state of metals by examining a wider class of superconductors which generally have values of γ^* much less than the materials listed in Table VII. We have examined the "d-band" superconductors and related compounds listed in Table VIII for two basic reasons. First, these materials have γ^* values whose magnitude falls roughly between the heavy-fermion compounds and simple metals such as Cu or Al, and include many high-T_c superconductors. Second, the bandwidths of many of the materials of Table VIII are generally sufficiently small so that large orbital contributions to χ may be expected, but not so small as to be dominated by the Pauli susceptibility. Therefore, these compounds provide a measure of the potential "decorrelating effect" of not explicitly separating out relatively sizeable χ_0^* contributions to the χ data.

Surprisingly, we have found that the $\mathscr{R}$ correlation of Table VII remains essentially intact over the significantly broader class of materials represented in Table VIII. The superconductors of Table VIII generally exhibit $\mathscr{R} \approx 2.0 \pm 0.5$, with few exceptions. Materials having $\mathscr{R} < 1.5$ generally also have relatively high γ^* and T_c values. Notable exceptions to these trends (particularly Nb_3Sb!) have lower T_c and γ^* values. This suggests that orbital contributions to $\mathscr{R}$ become significant for materials with $\gamma^* < 10$ mJ/K^2 g-at. Nevertheless, within a series of related compounds (viz., Ti_3Ir-Pt, V_3Au-Pt, Nb_3Os-Sb) the (anti)correlation of T_c with $\mathscr{R}$ is remarkably well obeyed.

There are two groups of materials which do not appear to simply obey the trends discussed above. The $B1$ structure compounds are low-γ^*, high-T_c materials with small χ and γ^* values which would imply that core diamagnetism and orbital effects could strongly affect their magnetic behavior. We note that VN, which has been dis-

TABLE VIII. Experimental values of the enhancement ratio of cubic, high-T_c superconductors and their relatives.

Compounds	Structure	χ (10^{-3} cm^3/mole)	γ^* (mJ/mole K^2)	$\mathscr{R}$	T_c (K)	References
Ti_3Ir	$A15$	0.604	6.34	1.7	4.3	128 and 129
Ti_3Pt	$A15$	0.564	5.67	1.8	0.49	128 and 129
Ti_3Au	$A15$	0.428	3.93	2.0	<0.015	128 and 129
V_3Au	$A15$	1.34	13.09	1.9	2.83	128 and 130
V_3Pt	$A15$	0.868	7.09	2.2	2.73	128 and 130
V_3Pd	$A15$	0.764	4.8	2.9	0.082	128
V_3Rh	$A15$	0.584	2.3	4.6	<0.015	128
V_3Ir	$A15$	0.532	1.94	5.0	<0.015	128 and 130
V_3Si	$A15$	1.54	62.8	1.8	17.0	131 and 132
V_3Ga	$A15$	1.80	96.9	1.35	15.0	130 and 133
Cr_3Ir	$A15$	1.04	8.4	2.3	0.168	128
Nb_3Os	$A15$	0.424	9.2	3.3	0.943	128 and 134
Nb_3Ir	$A15$	0.348	8.20	3.1	1.48	130 and 135
Nb_3Pt	$A15$	0.524	24.68	1.5	10.03	130 and 135
Nb_3Au	$A15$	0.656	36.8	1.3	10.59	134 and 135
Nb_3Al	$A15$	0.768	45.6	1.2	18.7	136
Nb_3Sn	$A15$	0.982	57.2	1.3	18.0	130 and 138
Nb_3Sb	$A15$	0.36	4.4	6.0	0.2	137 and 138
Mo_3Ir	$A15$	0.368	3.0	2.2	8.11	128
TiN	$B1$	0.038	3.3	0.8	5.5	128
ZrN	$B1$	0.022	2.7	0.6	10.0	128
VN	$B1$	0.144	9.6	1.1	8.6	134
NbN	$B1$	0.024	4.17	0.4	17.3	134
$LaSn_3$	$L1_2$	0.26	11.66	1.6	6.4	70 and 139—141
$LaPb_3$	$L1_2$	0.012	13.0	0.07	4.07	70 and 141
$LaIn_3$	$L1_2$	0.34	7.7	3.2	0.71	70 and 141
La_3Tl	$L1_2$	0.48	12.4	2.8	9.04	71
La_3In	$L1_2$	0.48	14.0	2.5	9.63	71

cussed as a possible spin-fluctuation compound,[68] has a somewhat higher γ^* and $\mathscr{R} > 1$. V_3Ga has also been proposed as a spin-fluctuation system,[45] and the modest value $\mathscr{R} \approx 1.35$ is still consistent with the upper critical-field data which have been interpreted in terms of strong Pauli limiting.[45,69] The $L1_2$ compounds also exhibit an irregular relationship between $\mathscr{R}$ and T_c. Arguments have been given for the presence of strong orbital contributions to χ in these materials[70,71] and this view may provide an explanation of the data in Table VIII.

The $\mathscr{R}$ correlation proves to be remarkably general, encompassing a much broader class of materials, with much less data manipulation, than has been previously recognized. It seems particularly well suited to materials for which $\gamma^* > 10$ mJ/K^2 g-at., presumably because the larger effective mass and/or the relative size of the Pauli susceptibility of these systems effectively suppresses the importance of orbital contributions to χ. For example, Fermi-surface measurements of $CeSn_3$ and Pd (inlcuded in Table VII) yield m^* values ($<10m_e$) which are much larger than those of $LaSn_3$ (included in Table VIII).[72] Future theories should attempt to identify the fundamental reasons for the trends discussed here.

Our primary motivation for introducing the $\mathscr{R}$ correlation was to assess the degree of exchange enhancement of χ in the U_6X materials and its influence on T_c. Our discussion indicates that U_6Mn and U_6Ni (for which $\gamma^* > 10$ mJ/K^2 g-at.) have a rather high value $\mathscr{R} \sim 2.25$ for heavy-fermion superconductors, and this would seem to indicate a significant exchange enhancement of χ rather than a large χ_0^*.

D. Comparison to pairing models

Recent calculations[36,37,73] have estimated the transition temperature to a triplet-paired superconducting state for U compounds. Landau theories[36,37] have suggested that U_6Fe and several other heavy-fermion materials are triplet superconductors with an isotropic, Balian-Werthamer (He-3B) ground state. They also show that the exchange enhancement $\mathscr{S}$ [as defined in Eq. (12)] cannot exceed 4—10, independent of the size of m^*/m_e, consistent with the analogous results for $\mathscr{R} \leq 6$ listed in Table VII. Bedell and Quader[37] have pointed out that a strong suppression of T_c is expected to occur due to an intensified competition between the electron-phonon and paramagnon interactions in situations where m^* is somewhat smaller than is the case for U_6Fe ($m^*/m_e \sim 20$). This effect should be maximal for T_0 (spin-fluctuation temperature) $\gtrsim \theta_D$ (Debye temperature). Valls and Tesanovic[36] place $T_0 \sim 40$ K for U_6Fe, where $\Theta_D \sim 100$ K.[1–3] The decrease of T_c below 3 K, accompanied by an increase of $\mathscr{R}$ to ~ 2.2 and a simultaneous decrease of m^*/m_e may be symptomatic of these effects occurring in U_6Mn and U_6Ni.

The interplay between heavy-fermion quasiparticles and phonons needs to be clarified for several reasons. The traditional models of BCS pairing rely upon the adiabatic adjustment of the Fermi liquid to the motion of the crystal lattice since the Fermi energy $E_F \gg k_B\Theta_D$. However, one can have $k_BT_0 < E_F < k_B\Theta_D$ in the case of heavy-fermion materials, whereupon Migdal's theorem is no longer valid.[74] This can lead to important modifications of the many-body correlations and associated physical properties.[75] For example, the influence of the electron-phonon interaction on the spin susceptibility has been estimated to be of order $\mathscr{S}k_B\Theta_D/E_F$ for $k_B\Theta_D \ll E_F$.[57,75] Such questions must be reexamined in the case of U_6X compounds where $k_B\Theta_D < E_F$, and it is also possible that $8 < \mathscr{S} < 70$.

There is also a need to investigate phonon as well as paramagnon pairing mechanisms in heavy-fermion materials.[75] Recent calculations based on the Anderson model have been applied to explain the superconductivity of $CeCu_2Si_2$ in terms of a phonon mechanism.[74,76–78] On the other hand, triplet pairing mediated by paramagnons has been favored by other authors.[36,37,73,75,79,80] Experimental evidence has been presented which favors triplet pairing in UBe_{13} (Refs. 73 and 81) and UPt_3 (Refs. 79, 80, and 82), but the analyses of these measurements are complicated and controversial.[83–85] Pals *et al.*[86] have observed Josephson oscillations in Nb point-contact junctions with U_6Fe, and argue that this constitutes strong evidence against odd-parity pairing in this compound. It is difficult to understand the superconductivity of U_6Fe if it is singlet paired *and* strongly exchange enhanced;[13,16,36,27] alternatively, it is puzzling that the $T_c \approx 3.8$ K for U_6Fe is so low considering the very large value of γ^* observed for this material,[1–3] especially if $\mathscr{S} \approx 1$. Additional work will be necessary to understand these materials. In particular, Tedrow *et al.*[69] have obtained an independent (but indirect) measurement of $\mathscr{S}$ from spin-polarized tunneling experiments on Al; however, this technique has not yet been widely applied to non-simple metals.

VII. SUMMARY

The U_6X (X=Mn, Fe, Co, Ni) compounds are found to have strongly-paramagnetic, weakly-temperature-dependent susceptibilities $\chi \sim 4\times10^{-4}$ cm^3/g-at. at low temperatures, comparable to $\chi(T=0) \approx 7\times10^{-4}$ cm^3/g-at. observed for the highly-exchange-enhanced paramagnet Pd.[87] There is some preliminary evidence for significant anisotropy of χ for U_6Fe, but single-crystal studies will be necessary to confirm this.

All U_6X samples measured exhibited a ferromagnetic transition in the range $150 \leq T \leq 200$ K. This anomaly has been attributed to the presence of $\sim$10–100 ppm of the sample U being present in a ferromagnetic impurity phase (such as U_2N_3, UH_3, or UFe_2) which would be common to all samples studied, independent of the particular X element involved. Evidence was also found for the presence of UO_x phases in various samples, and some sample degradation may have occurred in a few of our U_6Fe samples which were stored in room conditions over periods of many months. U_6Co samples were found to have strongly-field-dependent susceptibilities at room temperature.

Application of a paramagnon model to the low-temperature susceptibility data imply that all of the U_6X compounds are strongly exchange enhanced with Stoner factors $8 \lesssim \mathscr{S} \lesssim 70$. Large values of $\mathscr{S}$ are consistent with theoretical models of the superconducting upper critical field, although other discrepancies between these theories and experiment exist.

An empirical correlation has been established relating the ratio $\mathscr{R}$ [see Eq. (15)] to the low-temperature behavior of a very broad class of metallic solids. (We note that Meisner *et al.*[88] have recently discussed the low-temperature properties of UBe_{13}, UPt_3, U_2PtC_2, U_6Fe, and α-U in terms of a closely-related ratio, χ/χ_{calc}.) The definition of $\mathscr{R}$ has the specific advantages of not requiring a detailed knowledge of various contributions to the total susceptibility or the electronic specific heat, and is independent of the exact nature of band structure, the degree of d- or f-state localization, and crystal field or spin-orbit interaction effects. This correlation indicates that superconducting metals can be found when $\mathscr{R} \lesssim 2.0$, whereas ferromagnets generally exhibit values $\mathscr{R} \gtrsim 2.0$. The correlation implies that "improved" samples of $CeAl_3$ and $CeCu_6$ may yet be found to be superconducting, but that Pd is a very poor candidate for superconductivity. The values of $\mathscr{R}$ tabulated for a very broad class of materials are consistent with model predictions[36,37,73,75] which place an upper limit of $\mathscr{S} \approx 4$–10 in "Brinkman-Rice" Fermi liquids.

The U_6X compounds are found to be at the borderline between ferromagnetism and superconductivity in that they appear to be exchange-enhanced paramagnets with values $1.4 \leq \mathscr{R} \leq 2.25$, although this conclusion relies upon orbital paramagnetism being negligible. The decrease of T_c in the sequence U_6Fe-U_6Co-U_6Mn-U_6Ni correlates with a possible concomitant increase in $\mathscr{S}$ or T_0, also consistent with recent Fermi-liquid models.[37] Further investigation of the roles of phonons and orbital degrees of freedom in the magnetic and superconducting behavior of heavy-fermion compounds is necessary to clarify their physical properties.

ACKNOWLEDGMENTS

We are indebted to Dr. J. J. Engelhardt (deceased) for providing some of the samples studied, and for early interest and enthusiastic support of this work. We would like to thank R. Pereyra, Dr. B. Roof, and Dr. J. L. Smith of Los Alamos National Laboratory for their help in obtaining metallographic and structural analyses of particular samples, and Professor B. Deaver for his support and enthusiasm. We would like to thank Dr. K. Bedell, and Professor P. Boolchand, Professor B. N. Harmon, Professor J. G. Huber, Dr. A. Junod, Professor C. W. Kimball, Professor M. B. Maple, Professor T. P. Orlando, Dr. H. G. Smith, Dr. Z. Tesanovic, Professor J. Wilkins, and K. N. Yang for useful discussions and/or communication of their unpublished results. Research at the University of Kentucky was supported by a grant from Research Corporation. Research at the University of Virginia was supported by National Science Foundation Grant No. DMR-82-04365. Research at Tufts University was supported by National Science Foundation Grant No. DMR-82-03690, and work done at the Francis Bitter National Magnet Laboratory was supported by the National Science Foundation.

---

[*] Also at the Francis Bitter National Magnet Laboratory, Massachusetts Institute of Technology, Cambridge, MA 02139.

[†] Present address: Department of Physics, University of Rhode Island, Kingston, RI 02881

[‡] Present address: Center for Naval Analyses, 2000 North Beauregard St., P.O. Box 11280, Alexandria, VA 22311.

[1] L. E. DeLong, J. G. Huber, K. N. Yang, and M. B. Maple, Bull. Am. Phys. Soc. **27**, 157 (1982).

[2] L. E. DeLong, J. G. Huber, K. N. Yang, and M. B. Maple, in *Superconductivity in d- and f-Band Metals 1982,* edited by W. Buckel and W. Weber (Kernforschungszentrum Karlsruhe, Karlsruhe, Federal Republic of Germany, 1982), pp. 467–471.

[3] L. E. DeLong, J. G. Huber, K. N. Yang, and M. B. Maple, Phys. Rev. Lett. **51**, 312 (1983).

[4] T. E. Carone and L. E. DeLong, Bull. Am. Phys. Soc. **29**, 404 (1984).

[5] L. E. DeLong, T. E. Carone, and J. J. Engelhardt, in *High Pressure in Science and Technology,* edited by C. Homan, R. K. MacCrone, and E. Whalley (North-Holland, Amsterdam, 1984), Part I, pp. 47–50.

[6] A. Junod, D. Bichsel, and J. Muller, Helv. Phys. Acta. **52**, 580 (1979).

[7] B. Lachal, A. Junod, and J. Muller, J. Low Temp. Phys. **55**, 195 (1984).

[8] R. Flükiger, S. Foner, E. J. McNiff, Jr., and B. B. Schwartz, J. Magn. Magn. Mater. **11**, 186 (1979).

[9] T. P. Orlando, E. J. McNiff, Jr., S. Foner, and M. R. Beasley, Phys. Rev. B **19**, 545 (1979).

[10] M. Decroux, and Ø. Fischer, in *Superconductivity in Ternary Compounds II,* edited by M. B. Maple and Ø. Fischer (Springer, Berlin, 1982), pp. 57–98.

[11] B. S. Chandrasekhar and J. K. Hulm, J. Phys. Chem. Solids **7**, 259 (1958).

[12] H. H. Hill and B. T. Matthias, Phys. Rev. **168**, 464 (1968).

[13] N. F. Berk and J. R. Schrieffer, Phys. Rev. Lett. **17**, 433 (1966).

[14] S. Misawa, Phys. Lett. **32A**, 153 (1970).

[15] G. Barnea, J. Phys. F **7**, 315 (1977).

[16] K. Andres and M. A. Jensen, Phys. Rev. **165**, 533 (1968); M. A. Jensen and K. Andres, *ibid.* **165**, 545 (1968).

[17] B. W. Roberts, J. Phys. Chem. Ref. Data **5**, 581 (1976).

[18] D. J. Lam and A. T. Aldred, in *The Actinides: Electronic Structure and Related Properties,* edited by A. J. Freeman and J. B. Darby, Jr. (Academic, New York, 1974), Vol. I, pp. 109–179; W. J. Nellis and M. B. Brodsky, *ibid.*, Vol. II, pp. 265–288.

[19] P. Gordon, D. Sc. thesis, Massachusetts Institute of Technology, available as a United States Atomic Energy Commission Report No. AECU-1833, 1952 (unpublished).

[20] L. F. Bates and J. R. Mallard, Proc. Phys. Soc. London, Sect. B **63**, 520 (1950).

[21] V. V. Gann, A. I. Skvortsov, and A. van den Bosch, Phys. Status Solidi A **41**, 225 (1977).

[22] B. S. Deaver, T. J. Bucelot, and J. J. Finley, in *Future Trends in Superconductive Electronics,* edited by B. S. Deaver, C. M. Falco, J. H. Harris, and S. A. Wolf (AIP, New York, 1979), p. 58.

[23] J. J. Engelhardt, J. Phys. Chem. Solids **36**, 123 (1975).

[24] G. Lemon, P. Boolchand, M. Stevens, M. Marcuso, L. E. DeLong, and J. G. Huber, Bull. Am. Phys. Soc. **29**, 405 (1984), and unpublished.

[25] H. G. Smith and L. E. DeLong (unpublished results).

[26] W. E. Henry, Phys. Rev. **109**, 1976 (1958).

[27] S. K. Dhar, K. A. Gschneidner, Jr., and L. E. DeLong (unpublished results).

[28] P. Gordon and A. R. Kaufmann, J. Metals, Trans. AIME **188**, 182 (1950).

[29] F. Y. Fradin, C. W. Kimball, C. Strelecky, P. P. Vaishnava, and A. E. Dwight, Bull. Am. Phys. Soc. **29**, 404 (1984), and unpublished.

[30] K. N. Yang, M. B. Maple, L. E. DeLong, J. G. Huber, and A. Junod (unpublished).

[31] G. R. Stewart, Rev. Mod. Phys. **56**, 755 (1984).

[32] W. Franz, A. Giessel, F. Steglich, and D. Wohlleben, Z. Phys. B **31**, 7 (1978).

[33] G. Landgren, Y. Jugnet, J. F. Morar, A. J. Arko, Z. Fisk, J. L. Smith, H. R. Ott, and B. Reihl, Phys. Rev. B **29**, 493 (1984).

[34] E. Wuilloud, Y. Baer, H. R. Ott, Z. Fisk, and J. L. Smith, Phys. Rev. B **29**, 5228 (1984).

[35] H. R. Ott, H. Rudigier, Z. Fisk, and J. L. Smith, Phys. Rev. Lett. **50**, 1595 (1983).

[36] O. T. Valls and Z. Tesanovic, Phys. Rev. Lett. **53**, 1497 (1984).

[37] K. Bedell and K. F. Quader (unpublished).

[38] J. L. Smith and E. A. Kmetko, J. Less-Common Met. **90**, 83 (1983).

[39] S. Doniach and S. Engelsberg, Phys. Rev. Lett. **47**, 750 (1966).

[40] R. M. White, *Quantum Theory of Magnetism* (McGraw-Hill, New York, 1970), Chap. 4.

[41] C. M. Place and P. Rhodes, Phys. Status Solidi B **47**, 475 (1971).

[42] M. S. S. Brooks and P. J. Kelly, Phys. Rev. Lett. **51**, 1708 (1983).

[43] S. K. Misra, P. K. Misra, and S. D. Mahanti, Phys. Rev. B **26**, 1903 (1982).

[44] E. König and G. König, in *Landolt-Börnstein Numerical Data and Functional Relationships in Science and Technology—New Series,* edited by K. H. Hellwege (Springer, Berlin, 1976), Group II, Vol. 8, Supp. 1.

[45] T. P. Orlando and M. R. Beasley, Phys. Rev. Lett. **46**, 1598 (1981).

[46] P. B. Allen and R. C. Dynes, Phys. Rev. B **12**, 905 (1975).

[47] W. F. Brinkman and S. Engelsberg, Phys. Rev. **169**, 417 (1968).

[48] L. N. Hall, G. W. Crabtree, H. Aoki, L. E. DeLong, and K. A. Gschneidner, Jr., Bull. Am. Phys. Soc. **30**, 358 (1985).

[49] N. R. Werthamer, E. Helfand, and P. C. Hohenberg, Phys. Rev. **147**, 295 (1966).

[50] K. Maki, Phys. Rev. **148**, 362 (1966).

[51] K. Levin and O. T. Valls, Phys. Rep. **98**, 1 (1983).

[52] W. Brenig, H. J. Mikeska, and E. Riedel, Z. Phys. **206**, 439 (1967).

[53] D. J. Amit, J. W. Kane, and H. Wagner, Phys. Rev. Lett. **19**, 425 (1967).

[54] E. Riedel, Z. Phys. **210**, 403 (1968).

[55] D. Pines and P. Nozières, *The Theory of Quantum Liquids*

(Benjamin, New York, 1966), Vol. I.

[56] A. J. Leggett, Rev. Mod. Phys. **47**, 330 (1975).

[57] D. J. Kim, Solid State Commun. **34**, 963 (1980).

[58] P. Nozières, J. Low Temp. Phys. **17**, 31 (1974).

[59] K. G. Wilson, Rev. Mod. Phys. **47**, 773 (1975).

[60] H. Lustfeld and A. Bringer, Solid State Commun. **28**, 119 (1978).

[61] D. M. Newns and A. C. Hewson, J. Phys. F **10**, 2429 (1980).

[62] B. Batlogg, J. P. Remeika, A. S. Cooper, and Z. Fisk, Bull. Am. Phys. Soc. **29**, 404 (1984).

[63] H. G. Smith, N. Wakabayashi, W. P. Crummett, R. M. Nicklow, G. H. Lander, and E. S. Fisher, Phys. Rev. Lett. **44**, 1612 (1979).

[64] H. R. Ott, H. Rudigier, P. Delsing, and Z. Fisk, Phys. Rev. Lett. **52**, 1551 (1984).

[65] J. J. M. Franse, Helv. Phys. Acta **56**, 131 (1983).

[66] G. R. Stewart, Z. Fisk, J. O. Willis, and J. L. Smith, Phys. Rev. Lett. **52**, 679 (1984).

[67] R. P. Peters, Ch. Buchal, M. Kubota, R. M. Mueller, and F. Pobell, Phys. Rev. Lett. **53**, 1108 (1984).

[68] H. Rietschel, H. Winter, and W. Reichardt, Phys. Rev. B **22**, 4284 (1980).

[69] P. M. Tedrow, J. T. Kucera, D. Rainer, and T. P. Orlando, Phys. Rev. Lett. **52**, 1637 (1984).

[70] L. B. Welsh, A. M. Toxen, and R. J. Gambino, Phys. Rev. B **6**, 1677 (1972).

[71] P. Descouts, B. Perrin, A. Dupanloup, and A. Treyvaud, J. Phys. Chem. Solids **39**, 161 (1978).

[72] G. W. Crabtree, W. R. Johanson, A. S. Edelstein, and O. D. McMasters, in *Valence Fluctuations in Solids,* edited by L. M. Falicov, W. Hanke, and M. B. Maple (North-Holland, Amsterdam, 1981), pp. 93—97.

[73] H. R. Ott, H. Rudigier, T. M. Rice, K. Ueda, Z. Fisk, and J. L. Smith, Phys. Rev. Lett. **52**, 1915 (1984).

[74] N. Grewe, Z. Phys. B **56**, 111 (1984).

[75] P. W. Anderson, Phys. Rev. **30**, 1549 (1984).

[76] M. Tachiki and S. Maekawa, Phys. Rev. B **29**, 2497 (1984).

[77] H. Razafimandimby, P. Fulde, and J. Keller, Z. Phys. B **54**, 111 (1984).

[78] N. d'Ambrumenil and P. Fulde, J. Magn. Magn. Mater. (to be published).

[79] C. M. Varma (unpublished results); Bull. Am. Phys. Soc. **29**, 404 (1984).

[80] D. J. Bishop, C. M. Varma, B. Batlogg, E. Bucher, Z. Fisk, and J. L. Smith, Phys. Rev. Lett. **53**, 1009 (1984).

[81] D. E. MacLaughlin, C. Tien, W. G. Clark, M. D. Lan, Z. Fisk, J. L. Smith, and H. R. Ott, Phys. Rev. Lett. **53**, 1833 (1984).

[82] J. W. Chen, S. E. Lambert, M. B. Maple, Z. Fisk, J. L. Smith, G. R. Stewart, and J. O. Willis, Phys. Rev. B **30**, 1583 (1984).

[83] A. W. Overhauser and J. Appel, Phys. Rev. B **31**, 193 (1985).

[84] K. Scharnberg and R. A. Klemm (unpublished).

[85] L. P. Gor'kov, Pis'ma Zh. Eksp. Teor. Fiz. **40**, 351 (1984) [JETP Lett. **40**, 1155 (1984)].

[86] J. A. Pals, W. van Haeringen, and M. H. van Maaren, Phys. Rev. B **15**, 2592 (1977).

[87] W. Sänger and J. Voltländer, Z. Phys. B **38**, 133 (1980).

[88] G. P. Meisner, A. L. Giorgi, A. C. Lawson, G. R. Stewart, J. O. Willis, M. S. Wire, and J. L. Smith, Phys. Rev. Lett. **53**, 1829 (1984).

[89] G. R. Marpoe, Jr. and G. H. Lander, Solid State Commun. **26**, 599 (1978).

[90] V. Sechovsky, Z. Smetana, G. Hilscher, E. Gratz, and H. Sassik, Physica (Utrecht) **102B**, 277 (1980).

[91] J. M. Fournier, Solid State Commun. **29**, 111 (1979).

[92] A. Murasik, P. Fischer, and Z. Zolnierek, Physica (Utrecht) **102B**, 188 (1980).

[93] H. J. van Daal, K. H. J. Buschow, P. B. van Aken, and M. H. van Maaren, Phys. Rev. Lett. **34**, 1457 (1975).

[94] C. S. Barrett, M. H. Mueller, and R. L. Hitterman, Phys. Rev. **129**, 625 (1963).

[95] S. D. Bader, N. E. Phillips, and E. S. Fisher, Phys. Rev. **12**, 4929 (1975).

[96] J. C. Ho, N. E. Phillips, and T. F. Smith, Phys. Rev. Lett. **17**, 694 (1966).

[97] W. E. Gardner and T. F. Smith, Phys. Rev. **154**, 309 (1967).

[98] W. D. Schneider and C. Laubschat, Phys. Rev. B **23**, 997 (1981).

[99] G. R. Stewart, Z. Fisk, J. L. Smith, J. O. Willis, and M. S. Wire, Phys. Rev. B **30**, 1249 (1984).

[100] Z. Fisk, G. R. Stewart, J. O. Willis, H. R. Ott, and F. Hulliger, Phys. Rev. B **30**, 6360 (1984).

[101] M. H. van Maaren, H. J. van Daal, K. H. J. Buschow, and C. J. Schinkel, Solid State Commun. **14**, 145 (1974).

[102] A. Misiuk, J. Mulak, and A. Czopnik, Bull. Acad. Polonaise Sci., Ser. Sci. Chim. **20**, 459 (1972).

[103] R. J. Trainor, M. B. Brodsky, and H. V. Culbert, Phys. Rev. Lett. **34**, 1019 (1975).

[104] T. F. Smith, H. L. Luo, M. B. Maple, and I. R. Harris, J. Phys. F **1**, 896 (1971).

[105] R. R. Joseph, K. A. Gschneidner, Jr., and D. C. Koskimaki, Phys. Rev. B **6**, 3286 (1972).

[106] D. C. Koskimaki and K. A. Gschneidner, Jr., Phys. Rev. B **11**, 4463 (1975).

[107] W. H. Zachariasen, J. Appl. Phys. **48**, 1391 (1977).

[108] M. R. MacPherson, G. E. Everett, D. Wohlleben, and M. B. Maple, Phys. Rev. Lett. **26**, 20 (1971).

[109] N. E. Phillips, J. C. Ho, and T. F. Smith, Phys. Lett. **27A**, 49 (1968).

[110] C. Probst and J. Wittig, in *Handbook on the Chemistry and Physics of Rare Earths,* edited by K. A. Gschneidner, Jr. and L. Eyring (North-Holland, Amsterdam, 1978), Vol. 1, Chap. 10.

[111] W. Assmus, M. Herrmann, U. Rauchschwalbe, S. Riegel, W. Lieke, H. Spille, S. Horn, G. Weber, F. Steglich, and G. Cordier, Phys. Rev. Lett. **52**, 469 (1984).

[112] U. Rauchschwalbe, W. Lieke, F. Steglich, C. Godart, L. C. Gupta, and R. D. Parks, Phys. Rev. B **30**, 444 (1984).

[113] K. Andres, J. E. Graebner, and H. R. Ott, Phys. Rev. Lett. **35**, 1779 (1975).

[114] Y. Onuki, Y. Shimizu, and T. Komatsubara, J. Phys. Soc. Jpn. **53**, 1210 (1984).

[115] G. R. Stewart, Z. Fisk, and M. S. Wire, Phys. Rev. B **30**, 482 (1984).

[116] H. R. Ott, H. Rudigier, Z. Fisk, J. O. Willis, and G. R. Stewart, Solid State Commun. **53**, 235 (1985).

[117] J. P. Kappler and A. Meyer, J. Phys. F **9**, 143 (1979).

[118] J. R. Cooper, C. Rizzuto, and G. Olcese, J. Phys. (Paris) Colloq. **32**, C1-1136 (1971).

[119] T. W. E. Tsang, K. A. Gschneidner, Jr., O. D. McMasters, R. J. Stierman, and S. K. Dhar, Phys. Rev. B **29**, 4185 (1984).

[120] T. Mihalisin, P. Scorboria, and J. A. Ward, Phys. Rev. Lett. **46**, 862 (1981).

[121] I. R. Harris, M. Norman, and W. E. Gardner, J. Less-Common Met. **29**, 299 (1972).

[122] D. W. Budworth, F. E. Hoare, and J. Preston, Proc. R. Soc. London, Ser. A **257**, 250 (1960).

[123] J. Abart, W. Sänger, and J. Voitländer, J. Magn. Magn.

Mater. **28**, 282 (1982).

[124]Ch. Buchal, F. Pobell, R. M. Mueller, M. Kubota, and J. R. Owers-Bradley, Phys. Rev. Lett. **50**, 64 (1983).

[125]B. W. Veal and J. A. Rayne, Phys. Rev. **135**, A442 (1961).

[126]D. J. Lam, J. B. Darby, Jr., and M. V. Nevitt, in *The Actinides: Electronic Structure and Related Properties,* edited by A. J. Freeman and J. B. Darby (Academic, New York, 1974), Vol. II, Chap. 4.

[127]I. Iandelli and A. Palenzona, in *Handbook on the Chemistry and Physics of Rare Earths,* edited by K. A. Gschneidner, Jr. and L. Eyring (North-Holland, Amsterdam, 1979), Vol. 2, Chap. 1.

[128]D. I. Bardos, R. M. Waterstrat, T. J. Rowland, and J. B. Darby, Jr., J. Low Temp. Phys. **3**, 509 (1970).

[129]A. Junod, R. Flukiger, and J. Muller, J. Phys. Chem. Solids **37**, 27 (1976).

[130]A. Junod, T. Jarlborg, and J. Muller, Phys. Rev. B **27**, 1568 (1983).

[131]A. Handstein, B. Pietrass, and G. Behr, Phys. Status Solidi B **95**, 131 (1979).

[132]A. Junod and J. Muller, Solid State Commun. **36**, 721 (1980).

[133]A. Junod, R. Flükiger, A. Treyvaud, and J. Muller, Solid State Commun. **19**, 265 (1976).

[134]P. Spitzli, R. Flükiger, F. Heiniger, and J. Mueller, Phys. Lett. **30A**, 170 (1969).

[135]M. Bernasson, P. Descouts, R. Flükiger, and A. Treyvaud, Solid State Commun. **8**, 837 (1970).

[136]A. Junod, J. L. Jorda, M. Pelizzone, and J. Muller, Phys. Rev. B **29**, 1189 (1984).

[137]G. S. Knapp, S. D. Bader, and Z. Fisk, Phys. Rev. B **13**, 3783 (1976).

[138]G. W. Webb, Z. Fisk, and D. C. Johnston, Phys. Lett. **73A**, 350 (1979).

[139]L. E. DeLong, R. W. McCallum, W. A. Fertig, M. B. Maple, and J. G. Huber, Solid State Commun. **22**, 245 (1977).

[140]L. E. DeLong, M. Tovar, L. D. Woolf, M. B. Maple, D. C. Johnston, and J. Keller, J. Low Temp. Phys. **38**, 119 (1980).

[141]E. Bucher, K. Andres, J. P. Maita, and G. W. Hull, Jr., Helv. Phys. Acta **41**, 723 (1968).